Microstructural and metabolic alterations in the zebrafish brain induced by toll-like receptor 2 deficiency: insights from ultra-high field magnetic resonance imaging and spectroscopy

Singer, R.

6

CONCLUSIONS AND FUTURE OUTLOOK

Toll-like receptors (TLRs), and specifically TLR2, play a pivotal role in the immune system by recognizing pathogens and initiating inflammatory responses. However, there is growing evidence that TLR2 is also involved in the pathology of neurological disorders, acting as a double-edged sword. While TLR2's activation can help combat infections, its dysregulation may contribute to neuroinflammation and neurodegeneration. Despite its critical functions, the complete involvement of TLR2 in normal brain functioning remains poorly understood, necessitating further research to elucidate its complex roles in both health and disease.

Magnetic resonance (MR) techniques, including magnetic resonance imaging (MRI) and magnetic resonance spectroscopy (MRS), are non-invasive methods offering a broad range of information on the microstructural and biochemical environment of tissues. Utilizing the same basic principles of nuclear magnetic resonance (NMR), MRI provides detailed anatomical images and microstructural information through local relaxation times, while MRS delivers insights into the local chemical composition of tissue. Furthermore, diffusion-based MRI (dMRI), including diffusion-weighted imaging (DWI), diffusion tensor imaging (DTI), and dMRI tractography extends the capabilities of conventional MRI by measuring the random motion of water molecules within tissues. This allows for the visualization and characterisation of microstructural changes that are not apparent in standard MRI scans. The versatility of MRI data is largely dictated by the specific MR sequences employed, which can be utilized to provide specific tissue contrast, molecular interactions, and physiological processes, making MR techniques invaluable in both clinical and research settings.

The main scope of this thesis was the optimization and application of MRI and MRS techniques at ultra-high magnetic field (UHF) strengths to obtain non-invasive insights into microstructural and neurochemical changes in the zebrafish (*Danio rerio*) brain caused by TLR2 deficiency. Zebrafish have become a prevalent model for studying neurological diseases due to their rapid development, fast reproduction, low maintenance costs, straightforward husbandry, and the comprehensive availability of pathological models stemming from their fully sequenced genome. Despite their growing use in neuroscience research, the application of MRI and MRS to zebrafish has been scarcely explored. These advanced imaging techniques hold great potential for non-invasively investigating the structural and metabolic aspects of neurological conditions in zebrafish, providing new insights that complement traditional methods. However, the relative low sensitivity of MR based techniques in combination with the size of the zebrafish brain, has limited their application.

In this work, we have shown that utilization of UHFs in MRI and MRS, in combination with strong gradient systems up to 3 T/m (G_{max}) provides the necessary signal-to-noise ratio (SNR), spatial resolution, and contrasts required for detailed examination of zebrafish brain structures.

Fast spin echo MRI sequences at 28.2 T provide anatomical images with high tissue-contrast for the identification of a wide range of zebrafish brain structures, with additional contrast obtained through diffusion-weighted MRI (Chapter 2). Additionally, dMRI tractography through short-track track-density imaging using multi-shell multi-tissue constrained spherical deconvolution method (stTDI msmt CSD) provided super-resolution (5 µm) tractography maps of the zebrafish brain for the visualization of tiny white matter structures. In addition to MRI and dMRI, UHF systems significantly enhance the SNR and provide highly resolved spectra of localized brain regions through MRS in the zebrafish brain (Chapter 4). Localized MRS at UHF enables the acquisition of detailed spectra from very small regions, as small as 125 nL, in relatively short measurement times (~30 minutes). This capability is crucial for studying the zebrafish brain, allowing for precise metabolic profiling and improved understanding of neurochemical processes within these minute, localized areas. However, MR artifacts, and specifically chemical shift displacement effects escalate at UHF and need to be corrected. We have shown how these effects can be minimized through optimization of the excitation frequency and excitation- and refocussing RF pulse bandwidths.

We successfully applied these techniques to show TLR2 deficiency causes both microstructural (Chapter 3) and metabolic (Chapter 5) changes in the zebrafish brain. Brain tissue of *tlr2*$^{-/-}$ zebrafish showed significantly elevated transverse relaxation times (T_2) and decreased apparent diffusion coefficient (*ADC*), indicative of microstructural changes in the brain tissue and restricted diffusion, possibly indicative of neuroinflammation, cytotoxic edema, and astrogliosis. Furthermore, we observed significant changes in diffusion tensor and diffusion kurtosis metrics in several white matter structures in the *tlr2*$^{-/-}$ brain compared to a control group, indicative of neuronal damage. Additionally, high-resolution magic angle spinning (HR-MAS) spectroscopy of *tlr2*$^{-/-}$ and control zebrafish brain showed significant alterations in brain metabolites as a consequence of TLR2 deficiency. We report significant changes in the neurotransmitters glutamate and γ-aminobutyric acid (GABA), as well as changes in glutamine, involved in the glutamate/GABA-glutamine cycle. Furthermore, we observed significant changes in metabolites involved in the alanine-lactate cycle, indicative of increased cerebral energy utilization as a consequence of TLR2 deficiency. Utilizing localized MRS, cerebral metabolic profiles were obtained from the zebrafish forebrain, midbrain, and hindbrain, showing TLR2 deficiency causes an increase in lactate in all three major brain regions. Furthermore, significantly lower levels of N-acetyl aspartate (NAA) were found in the *tlr2*$^{-/-}$ hindbrain, indicative of diminished neuron integrity.

Our research on MRI and MRS at UHF demonstrates that these systems open innovative avenues for utilizing zebrafish in neurological research. By combining MRI, dMRI, and MRS data, we can comprehensively study both the microstructural and metabolic aspects of the

zebrafish brain. This integrated approach provides a broad and detailed field of research, enabling the investigation of neurological disorders with unprecedented precision. The high spatial resolution and enhanced SNR offered by UHF systems allow us to observe intricate brain structures and metabolic changes, thus facilitating a deeper understanding of the underlying mechanisms of neurological diseases in zebrafish models.

1. FUTURE OUTLOOK

The techniques presented in this study have the potential to be applied to other pathological zebrafish models, extending their utility beyond the current scope. Additionally, with the appropriate hardware for zebrafish imaging, these methods could be implemented *in vivo*, allowing for real-time observation and analysis. In this section preliminary results will be shared of a leptin-deficient zebrafish model, along with insights into how these techniques could be adapted for *in vivo* applications in future studies.

1.1 PROBING CORRELATION OF WM INTEGRITY AND FAT ACCUMULATION WITH UHF MRI

A biomedical field that could benefit significantly from UHF MRI and dMRI is the impact of body fat accumulation on brain health. Excessive body weight is a growing global health problem, with 39% of the global adult population being overweight and 13% of the global adult population developing obesity[1]. Excessive body weight, and especially obesity, significantly increases the risk of diminished health, including heart diseases[2], increases blood pressure[2], type 2 diabetes[3], liver diseases[4], fertility problems[5], and certain types of cancer[6,7]. Furthermore, recent studies showed a link between obesity and certain types of neurodegenerative diseases, including Alzheimer's disease and Parkinson's disease[8]. However, the precise mechanisms of increased body weight and the development of neurodegenerative diseases remains largely unclear.

Here, we present a pilot study demonstrating the utilization of a leptin-deficient (*lepb*$^{-/-}$) zebrafish model to monitor the effects of fat accumulation on brain microstructure and white matter integrity. Leptin is a hormone involved in the energy and appetite regulation[9]. A deficiency in leptin can cause insufficient leptin levels, leading to increased appetite and a decrease in the body energy expenditure[10]. Previously, we showed that leptin-deficiency in zebrafish causes significant fat infiltration in muscle tissue and muscle wasting [11]. However, the effects of the fat accumulation observed in *lepb*$^{-/-}$ zebrafish and the brain microstructure and neuronal health was not investigated. For the specific imaging of fat, MRI utilizes chemical shift selective imaging (cssi or CHESS)[12]. Cssi differs from regular anatomical imaging in MRI

by its ability to selectively image specific substances within the body based on their distinct resonance frequencies. While regular anatomical MRI produces images based on the overall signal from all tissues, cssi targets particular molecules, such as fat or water, by exploiting differences in their Larmor frequencies. In a pilot study, we utilized cssi to quantify the fat accumulation surrounding the brain and observed a significant increase in *lepb*$^{-/-}$ zebrafish compared to a control group (see Figure 6.1).

Utilizing DTI and dMRI tractography, our preliminary results show significant changes in the diffusivity and diffusion kurtosis of several white matter structures, indicating changes in the white matter microstructure (Figure 6.2). A direct correlation was found between the fat accumulation in the zebrafish head and several dMRI DTI and DKI metrics in white matter structures (see Table 6.1). Interestingly, we found significant changes in DTI and DKI metrics in the commissure of the secondary gustatory nuclei (Cgus) of *lepb*$^{-/-}$ zebrafish compared to a control group, as well as a negative correlation between the axial, radial, and mean diffusivity in the Cgus and the total fat accumulation in the zebrafish head. The Cgus is a neural pathway that connects the secondary gustatory nuclei on both sides of the zebrafish brain, playing a crucial role in processing taste-related information within the gustatory system[13]. Alterations

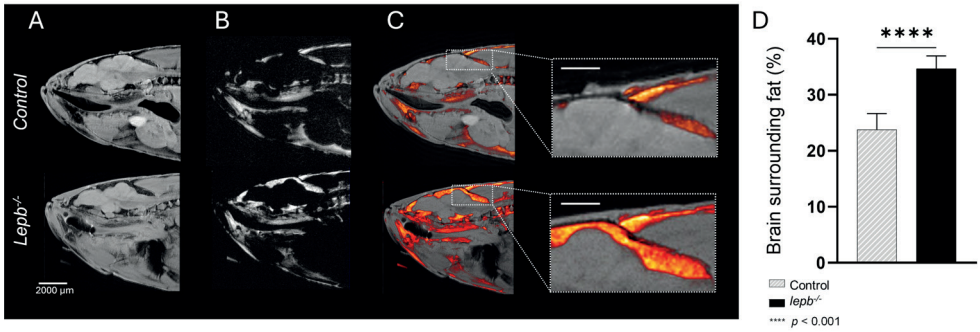

Figure 6.1. *Chemical shift selective imaging of the fat signal in control and lepb-deficient (lepb*$^{-/-}$*) adult zebrafish.* ***[A]*** *Representative sagittal slice of control and lepb*$^{-/-}$ *zebrafish measured by chemical shift selective imaging, selecting the water signal and* ***[B]*** *the fat signal.* ***[C]*** *Overlay of water signal (grey scale) and fat signal (hot colour scale) suggests increased distribution of fat in the head of lepb*$^{-/-}$ *adult zebrafish compared to control. This is elucidated in the zoomed view, shown in the right column. Scale bar in zoomed views indicate 500 µm.* ***[D]*** *Quantification of total area of fat (in %) surrounding brain tissue measured by chemical shift selective imaging. Data represents the mean value of the indicated MRI metric ± standard deviation (error bars). Statistical comparison between both groups performed by t-test, with a significant difference between the population means of control and lepb*$^{-/-}$ *assumed below the 0.05 level, **** p < 0.001. n = 3 and n = 6 for the control and lepb*$^{-/-}$ *groups, respectively. Cssi measurements were performed with a 17.6 T (750 MHz) vertical bore system (Bruker Biospin GmbH, Germany), configured with a Micro2.5 gradient system. Cssi sequence parameters TR = 1500 ms; TE = 12 ms; RARE factor = 4; ns = 4; resolution = 39 × 39 µm; slice thickness = 400 µm; Excitation pulse bandwidth = 2000 Hz.*

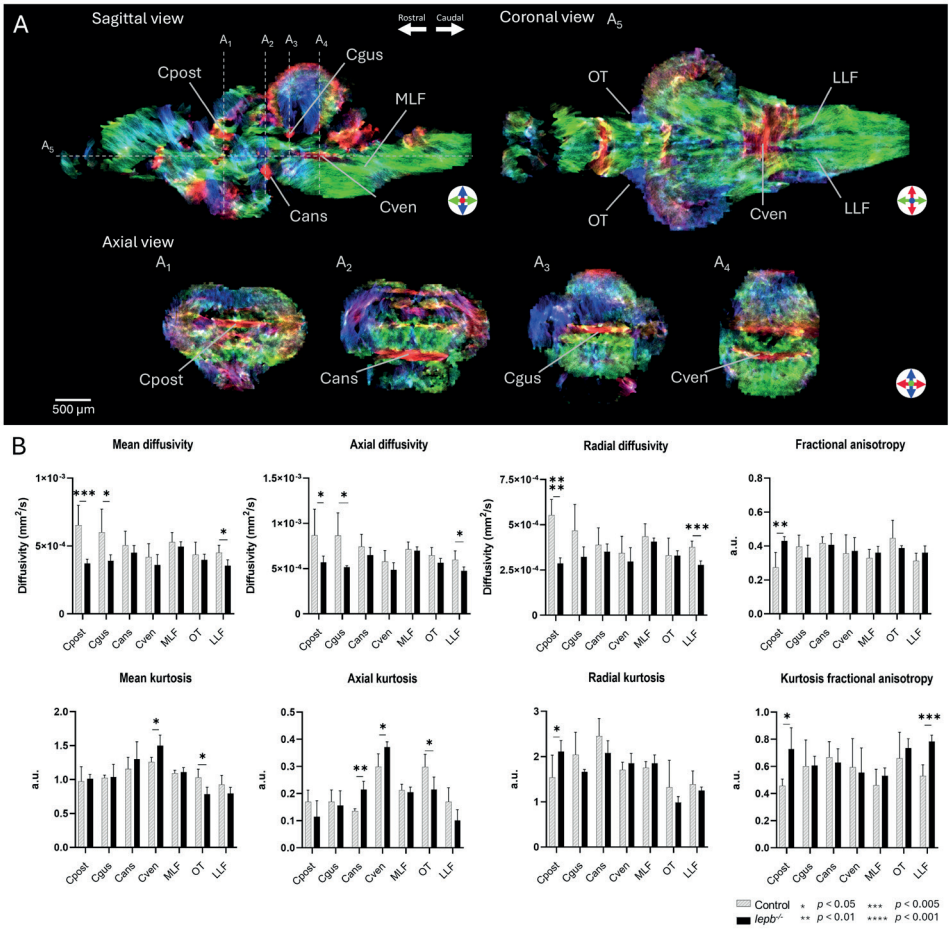

Figure 6.2. *Diffusion tensor imaging metrics and diffusion kurtosis imaging metrics of white matter structures in control and lepb-deficient (lepb$^{-/-}$) adult female zebrafish.* ***[A]*** *Sagittal (right top), coronal (left top) and axial (bottom row) slices of DEC stTDI msmt-CSD map, visualizing the exact location of various white matter structures in the zebrafish brain. Location of axial slices (A1 – A4) and coronal slice (A5) indicated in sagittal slice (dotted lines). Indicated white mater structures, Cpost – posterior commissure; Cgus – commissure of the secondary gustatory nuclei; Cans – ansulate commissure; Cven – ventral rhombencephalic commissure; MLF – medial longitudinal fascicle; OT – optic tract; LLF – lateral longitudinal fascicle.* ***[B]*** *Comparison of diffusion tensor metrics of white matter structures in control and lepb$^{-/-}$ zebrafish. Data represents the mean value of the indicated MRI metric ± standard deviation (error bars). Statistical comparison between both groups performed by t-test, with a significant difference between the population means of control and lepb$^{-/-}$ assumed below the 0.05 level, * p < 0.05, ** p < 0.01, *** p < 0.005, **** p < 0.001. n = 3 and n = 6 for the control and lepb$^{-/-}$ group, respectively. DTI measurements were performed with a 17.6 T (750 MHz) vertical bore system (Bruker Biospin GmbH, Germany), configured with a Micro2.5 gradient system. 3D DTI sequence parameters for white matter tractography TR = 1500 ms; TE = 17.3 ms; ns = 4, EPI factor = 7, δ = 1.5 ms, Δ = 10 ms, effective b-value range 160, 1000, or 2500 s/mm2 with 4, 12, or 24 diffusion encoding directions respectively, at an isotropic resolution of 45 µm. 2D DTI sequence parameters for DTI metric estimation TR = 1500 ms; TE = 22.8 ms; ns = 8, EPI factor = 20, δ = 1.5 ms, Δ = 15 ms, effective b-value range 2, 1000, 2500, or 4000 s/mm2 with 4, 12, 24, or 36 diffusion encoding directions respectively, at an isotropic resolution of 50 × 50 µm; slice thickness 300 µm.*

in this neural pathway could affect taste perception and preference, potentially influencing feeding behaviour and dietary choices. Understanding how obesity or increased body fat impacts the Cgus could provide insights into the neural mechanisms underlying altered eating behaviours and contribute to the development of interventions for overweight or obesity. Our research on the effects of fat accumulation and its correlation to changes in white matter integrity in the zebrafish brain demonstrates how UHF MRI and zebrafish models can be effectively utilized to study the impact of body fat on brain structure. This approach highlights the potential of these advanced imaging techniques and animal models to investigate the neural mechanisms underlying obesity and neurodegenerative diseases, providing valuable insights for developing targeted interventions.

1.2 IN VIVO APPLICATION OF MRI, DMRI, AND MRS METHODS AT UHFS

Shifting towards the *in vivo* application of MRI, dMRI, and MRS on zebrafish in pathological studies is crucial for advancing our understanding of neurological disorders in a living organism. *In vivo* imaging allows for the observation of dynamic biological processes and real-time monitoring of disease progression and response to treatments. This approach provides more

Table 6.1 *Statistical correlation analysis between fat infiltration (FI), as observed by cssi, and MR metrics estimated in the observed abnormality in the upper part of the rhombencephalon (see Fig.1A). Upward facing green arrows (↑) indicate significant (P_{corr} < 0.05) positive correlation (R > 0), while a downward facing red arrows (↓) indicate a significant(P_{corr} < 0.05) negative correlation (R < 0). A full overview of the statistical correlation analysis is found in the supplementary information S1. Cpost – posterior commissure; Cgus – commissure of the secondary gustatory nuclei; Cans – ansulate commissure; Cven – ventral rhombencephalic commissure; MLF – medial longitudinal fascicle; OT – optic tract; LLF – lateral longitudinal fascicle. To assess potential correlation between fat infiltration levels and MR metrics, we calculated correlation coefficients, based on the Pearson correlation method. Correlation coefficient values were subsequently cross-validated with their corresponding p values, excluding any correlation without statistical significance (p > 0.05). Potential outliers were detected and removed using a criterion based on three times the scaled median absolute deviation (MAD) from the median value.*

Metric *versus FI*	Cpost	Cgus	Cans	Cven	MLF	OT	LLF
MD	↓	↓	-	-	-	-	↓
$D_{\parallel}$	↓	↓	↓	-	-	-	↓
$D_{\perp}$	↓	↓	-	-	-	-	↓
FA	-	-	-	-	-	-	-
MK	-	-	-	-	-	-	↓
$K_{\parallel}$	-	-	↑	↑	-	-	↓
$K_{\perp}$	-	-	-	-	-	-	-
KFA	↑	-	-	-	-	-	↑

accurate and comprehensive insights into the physiological and metabolic changes occurring within the zebrafish brain, leading to more relevant and translatable findings for human health. Additionally, non-invasive *in vivo* imaging reduces the need for invasive procedures, thereby improving animal welfare and enabling longitudinal studies on the same subjects. This shift towards *in vivo* imaging necessitates specialised hardware to keep the zebrafish alive and under anaesthesia during the procedures[14]. Maintaining stable physiological conditions is essential to ensure accurate and reliable imaging results. Furthermore, to protect animal health, the applied imaging methods need to be as short as possible. This is particularly important if multiple imaging techniques are to be performed during the same session, allowing for precise comparison of different MRI methods within the same specimen.

Many of the high-resolution MR methods presented in this work meet the requirements for measurement time and could be adapted for *in vivo* applications with minimal modifications. However, translating our methods to *in vivo* applications necessitates consideration of the effects of formalin fixation on tissue relaxation times. It is well documented that formalin fixation shortens T_1 relaxation times, allowing for the use of shorter repetition times compared to *in vivo* conditions [15]. Therefore, applying our methods *in vivo* would require longer repetition times, resulting in extended total measurement times. This can be mitigated by reducing the number of scans, as our data indicate that the SNR is sufficient to maintain quality with fewer scans.

Nevertheless, not all presented MRI methods are suitable for *in vivo* application in their current state and require additional optimization. In particular, diffusion tensor imaging (DTI) and dMRI tractography inherently require long measurement times due to the numerous diffusion encoding orientations that must be recorded per voxel at multiple *b*-values. In clinical settings, single-shot EPI significantly reduces the total measurement time. However, the use of single-shot EPI for dMRI measurements on the zebrafish brain at UHFs is hindered by increased susceptibility artifacts. Although correction methods for susceptibility artifacts are available, they can cause significant changes in diffusion data, even in areas far from high distortion[16]. Potential solutions to shorten dMRI and dMRI tractography methods for *in vivo* applications include: (1) reducing the number of averages presented in the current work, albeit with additional noise; (2) reducing the applied resolution, which directly leads to shorter scan times due to fewer phase encoding gradient steps, while simultaneously increasing SNR per voxel, allowing for fewer scans per measurement and further decreasing the total measurement time; (3) further optimizing the number of diffusion encoding orientations and *b*-values beyond those presented in this work. However, for construction of accurate diffusion tensors, and especially diffusion kurtosis, it is recommended to use a high number of diffusion encoding orientations and *b*-values, which helps reduce noise and improve the accuracy of

the obtained diffusion metrics[17]; (4) significantly improving the obtained SNR per scan through the use of cryoprobe technology. As previously demonstrated for anatomical images of the zebrafish brain at 9.4 T (400 MHz), cryoprobe technology improved the SNR by a factor of 3 to 4, potentially shortening the total measurement time by a factor of 16[18].

REFERENCES

1 Organization, W. H. Obesity and overweight. (2017).

2 Klein, B. E. K., Cornoni, J. C., Jones, F. & Boyle, E. Overweight Indices as Correlates of Coronary Heart Diseases and Blood Pressure. *Human Biology* **45**, 329-340 (1973).

3 Long-term effects of lifestyle intervention or metformin on diabetes development and microvascular complications over 15-year follow-up: the Diabetes Prevention Program Outcomes Study. *Lancet Diabetes Endocrinol* **3**, 866-875 (2015). https://doi.org/10.1016/s2213-8587(15)00291-0

4 Hart, C. L., Batty, G. D., Morrison, D. S., Mitchell, R. J. & Smith, G. D. Obesity, overweight and liver disease in the Midspan prospective cohort studies. *International Journal of Obesity* **34**, 1051-1059 (2010). https://doi.org/10.1038/ijo.2010.20

5 Best, D. & Bhattacharya, S. Obesity and fertility. *Hormone Molecular Biology and Clinical Investigation* **24**, 5-10 (2015). https://doi.org/doi:10.1515/hmbci-2015-0023

6 Brawer, R., Brisbon, N. & Plumb, J. Obesity and cancer. *Primary Care: Clinics in Office Practice* **36**, 509-531 (2009).

7 Calle, E. E., Rodriguez, C., Walker-Thurmond, K. & Thun, M. J. Overweight, obesity, and mortality from cancer in a prospectively studied cohort of US adults. *New England Journal of Medicine* **348**, 1625-1638 (2003).

8 Kueck, P. J., Morris, J. K. & Stanford, J. A. Current Perspectives: Obesity and Neurodegeneration - Links and Risks. *Degener Neurol Neuromuscul Dis* **13**, 111-129 (2023). https://doi.org/10.2147/dnnd.S388579

9 Gorissen, M., Flik, G. & Huising, M. Peptides and proteins regulating food intake: a comparative view. *Animal Biology* **56**, 447-473 (2006). https://doi.org/https://doi.org/10.1163/157075606778967829

10 Cui, H., López, M. & Rahmouni, K. The cellular and molecular bases of leptin and ghrelin resistance in obesity. *Nat Rev Endocrinol* **13**, 338-351 (2017). https://doi.org/10.1038/nrendo.2016.222

11 Eeza, M. N. H. *et al.* Probing microstructural changes in muscles of leptin-deficient zebrafish by non-invasive ex-vivo magnetic resonance microimaging. *PLoS One* **18**, e0284215 (2023). https://doi.org/10.1371/journal.pone.0284215

12 Haase, A., Frahm, J., Hänicke, W. & Matthaei, D. 1H NMR chemical shift selective (CHESS) imaging. *Phys Med Biol* **30**, 341-344 (1985). https://doi.org/10.1088/0031-9155/30/4/008

13 Yanez, J., Souto, Y., Pineiro, L., Folgueira, M. & Anadon, R. Gustatory and general visceral centers and their connections in the brain of adult zebrafish: a carbocyanine dye tract-tracing study. *J Comp Neurol* **525**, 333-362 (2017). https://doi.org/10.1002/cne.24068

14 Kabli, S., Alia, A., Spaink, H. P., Verbeek, F. J. & De Groot, H. J. Magnetic resonance microscopy of the adult zebrafish. *Zebrafish* **3**, 431-439 (2006). https://doi.org/10.1089/zeb.2006.3.431

15 Birkl, C. *et al.* Effects of formalin fixation and temperature on MR relaxation times in the human brain. *NMR Biomed* **29**, 458-465 (2016). https://doi.org/10.1002/nbm.3477

16 Begnoche, J. P. *et al.* EPI susceptibility correction introduces significant differences far from local areas of high distortion. *Magnetic Resonance Imaging* **92**, 1-9 (2022). https://doi.org/https://doi.org/10.1016/j.mri.2022.05.016

17 Jones, D. K. The effect of gradient sampling schemes on measures derived from diffusion tensor MRI: a Monte Carlo study. *Magnetic Resonance in Medicine: An Official Journal of the International Society for Magnetic Resonance in Medicine* **51**, 807-815 (2004).

18 Kabli, S. *In vivo high field magnetic resonance imaging and spectroscopy of adult zebrafish*. (Leiden University, 2009).